
8 Polymer Nanocomposites

Polymer nanocomposites are polymer matrix composites in which the reinforcement has at least one of its dimensions in the nanometer range (1 nanometer (nm) = 10^{-3} μm (micron) = 10^{-9} m). These composites show great promise not only in terms of superior mechanical properties, but also in terms of superior thermal, electrical, optical, and other properties, and, in general, at relatively low-reinforcement volume fractions. The principal reasons for such highly improved properties are (1) the properties of nano-reinforcements are considerably higher than the reinforcing fibers in use and (2) the ratio of their surface area to volume is very high, which provides a greater interfacial interaction with the matrix.

In this chapter, we discuss three types of nanoreinforcements, namely nanoclay, carbon nanofibers, and carbon nanotubes. The emphasis here will be on the improvement in the mechanical properties of the polymer matrix. The improvement in other properties is not discussed in this chapter and can be found in the references listed at the end of this chapter.

8.1 NANOCCLAY

The reinforcement used in nanoclay composites is a layered silicate clay mineral, such as smectite clay, that belongs to a family of silicates known as 2:1 phyllosilicates [1]. In the natural form, the layered smectite clay particles are 6–10 μm thick and contain >3000 planar layers. Unlike the common clay minerals, such as talc and mica, smectite clay can be exfoliated or delaminated and dispersed as individual layers, each ~ 1 nm thick. In the exfoliated form, the surface area of each nanoclay particle is ~ 750 m^2/g and the aspect ratio is > 50 .

The crystal structure of each layer of smectite clays contains two outer tetrahedral sheets, filled mainly with Si, and a central octahedral sheet of alumina or magnesia (Figure 8.1). The thickness of each layer is ~ 1 nm, but the lateral dimensions of these layers may range from 200 to 2000 nm. The layers are separated by a very small gap, called the interlayer or the gallery. The negative charge, generated by isomorphic substitution of Al^{3+} with Mg^{2+} or Mg^{2+} with Li^+ within the layers, is counterbalanced by the presence of hydrated alkaline cations, such as Na or Ca, in the interlayer. Since the forces that hold the layers together are relatively weak, it is possible to intercalate small organic molecules between the layers.

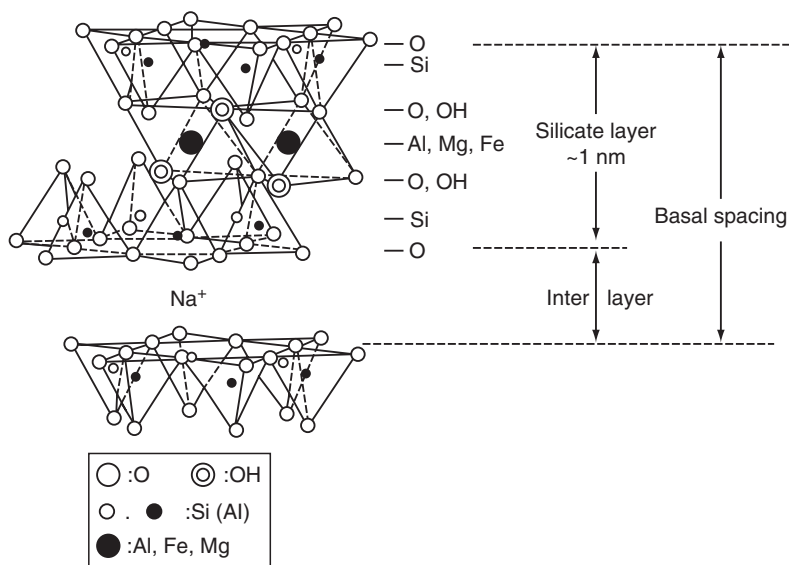
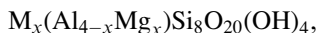


FIGURE 8.1 Crystal structure of smectite clay. (From Kato, M. and Usuki, A., *Polymer-Clay Nanocomposites*, T.J. Pinnavai and Beall, eds., John Wiley & Sons, Chichester, U.K., 2000. With permission.)

One of the common smectite clays used for nanocomposite applications is called montmorillonite that has the following chemical formula



where M represents a monovalent cation, such as a sodium ion, and x is the degree of isomorphous substitution (between 0.5 and 1.3). Montmorillonite is hydrophilic which makes its exfoliation in conventional polymers difficult. For exfoliation, montmorillonite is chemically modified to exchange the cations with alkyl ammonium ions. Since the majority of the cations are located inside the galleries and the alkyl ammonium ions are bulkier than the cations, the exchange increases the interlayer spacing and makes it easier for intercalation of polymer molecules between the layers.

When modified smectite clay is mixed with a polymer, three different types of dispersion are possible. They are shown schematically in [Figure 8.2](#). The type of dispersion depends on the polymer, layered silicate, organic cation, and the method of preparation of the nanocomposite.

1. Intercalated dispersion, in which one or more polymer molecules are intercalated between the silicate layers. The resulting material has a well-ordered multilayered morphology of alternating polymer and silicate layers. The spacing between the silicate layers is between 2 and 3 nm.

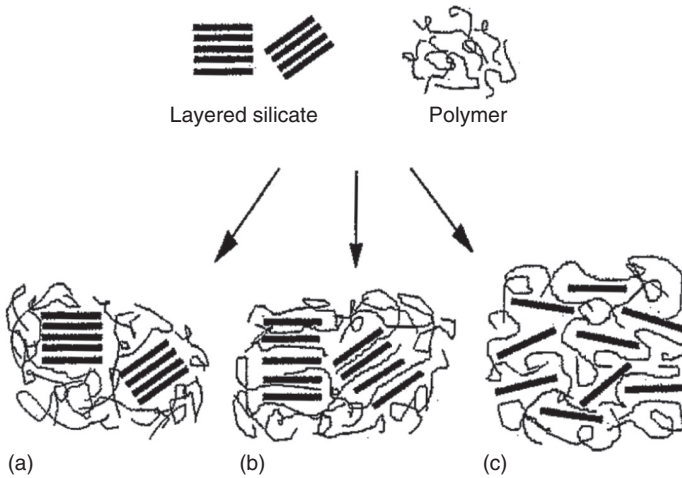


FIGURE 8.2 Three possible dispersions of smectite clay in polymer matrix. (a) phase-separated (microcomposite); (b) intercalated (nanocomposite); and (c) exfoliated (nanocomposite). (From Alexandre, M. and Dubois, P., *Mater. Sci. Eng.*, 28, 1, 2000. With permission.)

2. Exfoliated dispersion, in which the silicate layers are completely delaminated and are uniformly dispersed in the polymer matrix. The spacing between the silicate layers is between 8 and 10 nm. This is the most desirable dispersion for improved properties.
3. Phase-separated dispersion, in which the polymer is unable to intercalate the silicate sheets and the silicate particles are dispersed as phase-separated domains, called tactoids.

Following are the most common techniques used for dispersing layered silicates in polymers to make nanoclay–polymer composites.

1. *Solution method*: In this method, the layered silicate is first exfoliated into single layers using a solvent in which the polymer is soluble. When the polymer is added later, it is adsorbed into the exfoliated sheets, and when the solvent is evaporated, a multilayered structure of exfoliated sheets and polymer molecules sandwiched between them is created. The solution method has been widely used with water-soluble polymers, such as polyvinyl alcohol (PVA) and polyethylene oxide.
2. *In situ polymerization method*: In this method, the layered silicate is swollen within the liquid monomer, which is later polymerized either by heat or by radiation. Thus, in this method, the polymer molecules are formed in situ between the intercalated sheets.

The in situ method is commonly used with thermoset polymers, such as epoxy. It has also been used with thermoplastics, such as polystyrene and polyamide-6 (PA-6), and elastomers, such as polyurethane and thermoplastic polyolefins (TPOs). The first important commercial application of nanoclay composite was based on polyamide-6, and as disclosed by its developer, Toyota Motor Corp., it was prepared by the in situ method [2]. In this case, the montmorillonite clay was mixed with an α,ω -amino acid in aqueous hydrochloric acid to attach carboxyl groups to the clay particles. The modified clay was then mixed with the caprolactam monomer at 100°C, where it was swollen by the monomer. The carboxyl groups initiated the ring-opening polymerization reaction of caprolactam to form polyamide-6 molecules and ionically bonded them to the clay particles. The growth of the molecules caused the exfoliation of the clay particles.

3. *Melt processing method:* The layered silicate particles are mixed with the polymer in the liquid state. Depending on the processing condition and the compatibility between the polymer and the clay surface, the polymer molecules can enter into the interlayer space of the clay particles and can form either an intercalated or an exfoliated structure.

The melt processing method has been used with a variety of thermoplastics, such as polypropylene and polyamide-6, using conventional melt processing techniques, such as extrusion and injection molding. The high melt viscosity of thermoplastics and the mechanical action of the rotating screw in an extruder or an injection-molding machine create high shear stresses which tend to delaminate the original clay stack into thinner stacks. Diffusion of polymer molecules between the layers in the stacks then tends to peel the layers away into intercalated or exfoliated form [3].

The ability of smectite clay to greatly improve mechanical properties of polymers was first demonstrated in the research conducted by Toyota Motor Corp. in 1987. The properties of the nanoclay–polyamide-6 composite prepared by the in situ polymerization method at Toyota Research are given in [Table 8.1](#). With the addition of only 4.2 wt% of exfoliated montmorillonite nanoclay, the tensile strength increased by 55% and the tensile modulus increased by 91% compared with the base polymer, which in this case was a polyamide-6. The other significant increase was in the heat deflection temperature (HDT). [Table 8.1](#) also shows the benefit of exfoliation as the properties with exfoliation are compared with those without exfoliation. The nonexfoliated clay–PA-6 composite was prepared by simply melt blending montmorillonite clay with PA-6 in a twin-screw extruder.

Since the publication of the Toyota research results, the development of nanoclay-reinforced thermoplastics and thermosets has rapidly progressed.

TABLE 8.1
Properties of Nanoclay-Reinforced Polyamide-6

	Wt% of Clay	Tensile Strength (MPa)	Tensile Modulus (GPa)	Charpy Impact Strength (kJ/m²)	HDT (°C) at 145 MPa
Polyamide-6 (PA-6)	0	69	1.1	2.3	65
PA-6 with exfoliated nanoclay	4.2	107	2.1	2.8	145
PA-6 with nonexfoliated clay	5.0	61	1.0	2.2	89

Source: Adapted from Kato, M. and Usuki, A., in *Polymer–Clay Nanocomposites*, T.J. Pinnavaai and G.W. Beall, eds., John Wiley & Sons, Chichester, UK, 2000.

The most attractive attribute of adding nanoclay to polymers has been the improvement of modulus that can be attained with only 1–5 wt% of nanoclay. There are many other advantages such as reduction in gas permeability and increase in thermal stability and fire retardancy [1,4]. The key to achieving improved properties is the exfoliation. Uniform dispersion of nanoclay and interaction between nanoclay and the polymer matrix are also important factors, especially in controlling the tensile strength, elongation at break, and impact resistance.

8.2 CARBON NANOFIBERS

Carbon nanofibers are produced either in vapor-grown form [5] or by electrospinning [6]. Vapor-grown carbon nanofibers (VGCNF) have so far received the most attention for commercial applications and are discussed in this section. They are typically 20–200 nm in diameter and 30–100 μm in length. In comparison, the conventional PAN or pitch-based carbon fibers are 5–10 μm in diameter and are produced in continuous length. Carbon fibers are also made in vapor-grown form, but their diameter is in the range of 3–20 μm .

VGCNF are produced in vapor phase by decomposing carbon-containing gases, such as methane (CH_4), ethane (C_2H_6), acetylene (C_2H_2), carbon monoxide (CO), benzene, or coal gas in presence of floating metal catalyst particles inside a high-temperature reactor. Ultrafine particles of the catalyst are either carried by the flowing gas into the reactor or produced directly in the reactor by the decomposition of a catalyst precursor. The most common catalyst is iron, which is produced by the decomposition of ferrocene, $\text{Fe}(\text{CO})_5$. A variety of other catalysts, containing nickel, cobalt, nickel–iron, and nickel–cobalt compounds, have also been used. Depending on the carbon-containing gas, the

decomposition temperature can range up to 1200°C. The reaction is conducted in presence of other gases, such as hydrogen sulfide and ammonia, which act as growth promoters. Cylindrical carbon nanofibers grow on the catalyst particles and are collected at the bottom of the reactor. Impurities on their surface, such as tar and other aromatic hydrocarbons, are removed by a subsequent process called pyrolytic stripping, which involves heating them to about 1000°C in a reducing atmosphere. Heat treatment at temperatures up to 3000°C is used to graphitize their surface and achieve higher tensile strength and tensile modulus. However, the optimum heat treatment temperature for maximum mechanical properties is found to be close to 1500°C [5].

The diameter of carbon nanofibers and the orientation of graphite layers in carbon nanofibers with respect to their axis depend on the carbon-containing gas, the catalyst type, and the processing conditions, such as gas flow rate and temperature [7,8]. The catalyst particle size also influences the diameter.

Several different morphologies of carbon nanofibers have been observed [8,9]: platelet, in which the graphite layers are stacked normal to the fiber axis; hollow tubular construction, in which the graphite layers are parallel to the fiber axis, and fishbone or herringbone (with or without a hollow core), in which graphite layers are at an angle between 10° and 45° with the fiber axis (Figure 8.3). Single-wall and double-wall morphologies have been observed in heat-treated carbon nanofibers [10]. Some of the graphite layers in both single-wall and double-wall morphologies are folded, the diameter of the folds remaining close to 1 nm.

Table 8.2 lists the properties of a commercial carbon nanofiber (Pyrograf III) (Figure 8.4) as reported by its manufacturer (Applied Sciences, Inc.). The tensile modulus value listed in Table 8.2 is 600 GPa; however it should be noted that owing to the variety of morphologies observed in carbon nanofibers, they exhibit a range of modulus values, from as low as 110 GPa to as high as 700 GPa. Studies on vapor-grown carbon fibers (VGCF) [11], which are an order of

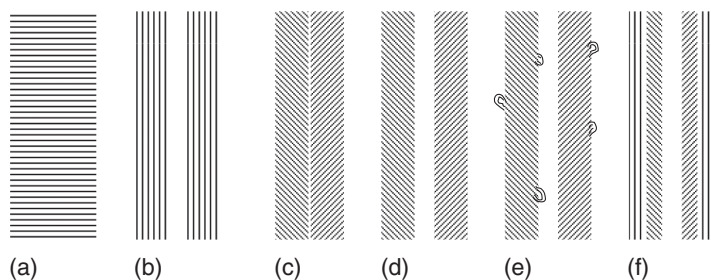


FIGURE 8.3 Different morphologies of carbon nanofibers. (a) Graphite layers stacked normal to the fiber axis; (b) Hollow tubular construction with graphite layers parallel to the fiber axis; (c) and (d) Fishbone or herringbone morphology with graphite layers at an angle with the fiber axis; (e) Fishbone morphology with end loops; and (f) Double-walled morphology.

TABLE 8.2
Properties of Vapor-Grown Carbon Nanofibers

Properties	Carbon Nanofibers ^a
	Pyrolytically Stripped
Diameter (nm)	60–200
Density (g/cm ³)	1.8
Tensile Modulus (GPa)	600
Tensile Strength (GPa)	7
Coefficient of thermal expansion (10 ⁻⁶ /°C)	-1.0
Electrical resistivity (μΩ cm)	55

^a Pyrograf III, produced by Applied Sciences, Inc.

magnitude larger in diameter than the VGCNF, have shown that tensile modulus decreases with increasing diameter, whereas tensile strength decreases with both increasing diameter and increasing length.

Carbon nanofibers have been incorporated into several different thermoplastic and thermoset polymers. The results of carbon nanofiber addition on the mechanical properties of the resulting composite have been mixed.

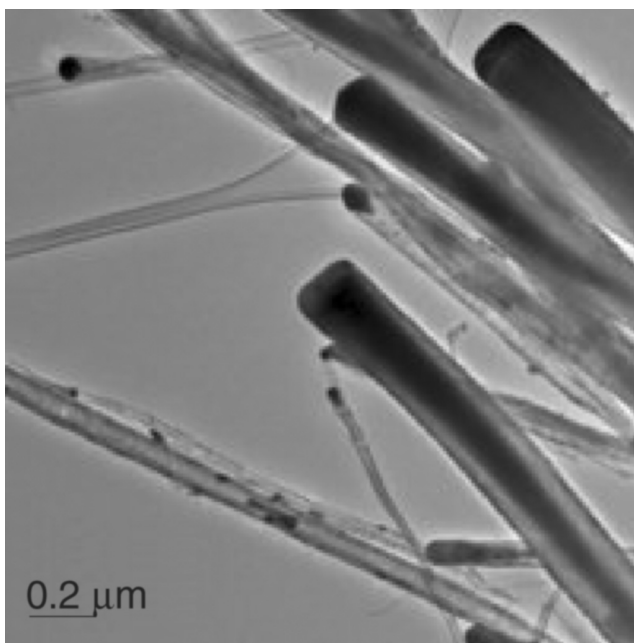


FIGURE 8.4 Photograph of carbon nanofibers. (Courtesy of Applied Sciences, Inc. With permission.)

In general, incorporation of carbon nanofibers in thermoplastics has shown modest to high improvement in modulus and strength, whereas their incorporation in thermosets has shown relatively smaller improvements. An example of each is given as follows.

Finegan et al. [12] conducted a study on the tensile properties of carbon nanofiber-reinforced polypropylene. The nanofibers were produced with a variety of processing conditions (different carbon-containing gases, different gas flow rates, with and without graphitization). A variety of surface treatments were applied on the nanofibers. The composite tensile specimens with 15 vol% nanofibers were prepared using melt processing (injection molding). In all cases, they observed an increase in both tensile modulus and strength compared with polypropylene itself. However, the amount of increase was influenced by the nanofiber production condition and the surface treatment. When the surface treatment involved surface oxidation in a CO₂ atmosphere at 850°C, the tensile modulus and strength of the composite were 4 GPa and 70 MPa, respectively, both of which were greater than three times the corresponding values for polypropylene.

Patton et al. [13] reported the effect of carbon nanofiber addition to epoxy. The epoxy resin was diluted using acetone as the solvent. The diluted epoxy was then infused into the carbon nanofiber mat. After removing the solvent, the epoxy-soaked mat was cured at 120°C and then postcured. Various nanofiber surface treatments were tried. The highest improvement in flexural modulus and strength was observed with carbon nanofibers that were heated in air at 400°C for 30 min. With ~18 vol% of carbon nanofibers, the flexural modulus of the composite was nearly twice that of epoxy, but the increase in flexural strength was only about 36%.

8.3 CARBON NANOTUBES

Carbon nanotubes were discovered in 1991, and within a short period of time, have attracted a great deal of research and commercial interest due to their potential applications in a variety of fields, such as structural composites, energy storage devices, electronic systems, biosensors, and drug delivery systems [14]. Their unique structure gives them exceptional mechanical, thermal, electrical, and optical properties. Their elastic modulus is reported to be >1 TPa, which is close to that of diamond and 3–4 times higher than that of carbon fibers. They are thermally stable up to 2800°C in vacuum; their thermal conductivity is about twice that of diamond and their electric conductivity is 1000 times higher than that of copper.

8.3.1 STRUCTURE

Carbon nanotubes are produced in two forms, single-walled nanotubes (SWNT) and multiwalled nanotubes (MWNT). SWNT is a seamless hollow cylinder and can be visualized as formed by rolling a sheet of graphite layer,

whereas MWNT consists of a number of concentric SWNT. Both SWNT and MWNT are closed at the ends by dome-shaped caps. The concentric SWNTs inside an MWNT are also end-capped. The diameter of an SWNT is typically between 1 and 1.4 nm and its length is between 50 and 100 μm . The specific surface area of an SWNT is 1315 m^2/g , and is independent of its diameter [15]. The outer diameter of an MWNT is between 1.4 and 100 nm. The separation between the concentric SWNT cylinders in an MWNT is about 3.45 \AA , which is slightly greater than the distance between the graphite layers in a graphite crystal. The specific surface area of an MWNT depends on the number of walls. For example, the specific surface area of a double-walled nanotube is between 700 and 800 m^2/g and that of a 10-walled nanotube is about 200 m^2/g [15].

The structure of an SWNT depends on how the graphite sheets is rolled up and is characterized by its chirality or helicity, which is defined by the chiral angle and the chiral vector (Figure 8.5). The chiral vector is written as

$$\mathbf{C}_h = n\mathbf{a}_1 + m\mathbf{a}_2, \quad (8.1)$$

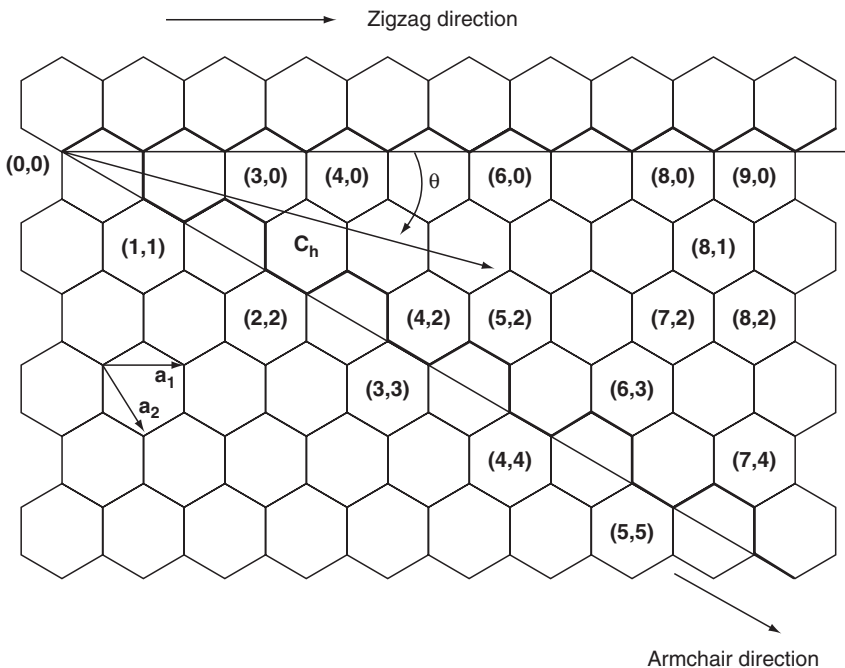


FIGURE 8.5 Chiral vector and chiral angle. (From Govindaraj, A. and Rao, C.N.R., *The Chemistry of Nanomaterials*, Vol. 1, C.N.R. Rao, A. Müller, and A.K. Cheetham, eds., Wiley-VCH, KGaA, Germany, 2004. With permission.)

where \mathbf{a}_1 and \mathbf{a}_2 are unit vectors in a two-dimensional graphite sheet and (n, m) are called chirality numbers. Both n and m are integers and they define the way the graphite sheet is rolled to form a nanotube.

Nanotubes with $n \neq 0, m = 0$ are called the zigzag tubes (Figure 8.6a) and nanotubes with $n = m \neq 0$ are called armchair tubes (Figure 8.6b). In zigzag tubes, two opposite C–C bonds of each hexagon are parallel to the tube’s axis, whereas in the armchair tubes, the C–C bonds of each hexagon are perpendicular to the tube’s axis. If the C–C bonds are at an angle with the tube’s axis, the tube is called a chiral tube (Figure 8.6c). The chiral angle θ is defined as the angle between the zigzag direction and the chiral vector, and is given by

$$\theta = \tan^{-1} \left[\frac{3^{1/2}m}{2n + m} \right] \tag{8.2}$$

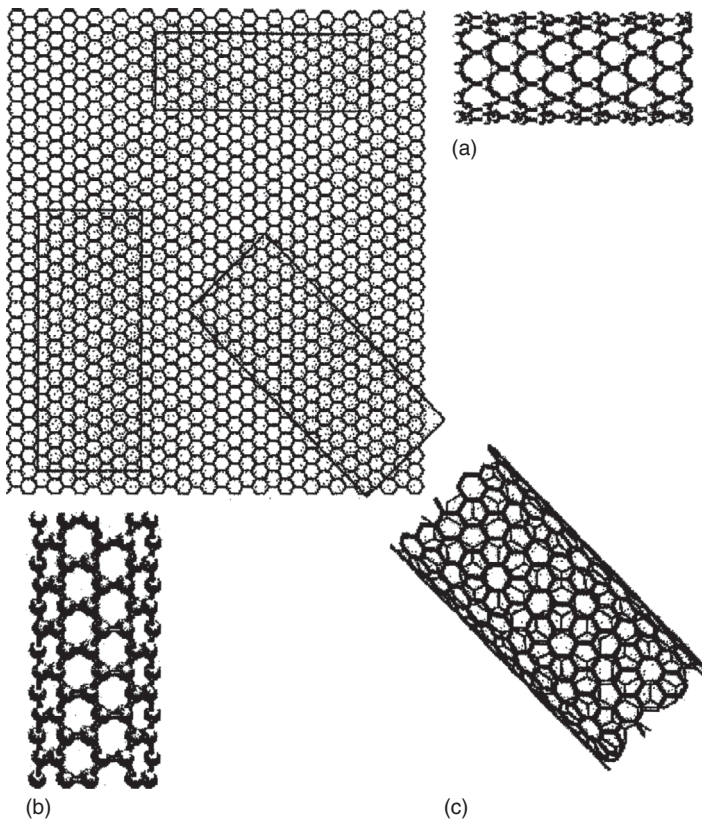


FIGURE 8.6 (a) Zigzag, (b) armchair, and (c) chiral nanotubes. (From Rakov, E.G., *Nanomaterials Handbook*, Y. Gogotsi, ed., CRC Press, Boca Raton, USA, 2006. With permission.)

and $0^\circ \leq \theta \leq 30^\circ$. The diameter of the nanotube is given by

$$d = \frac{a_o\sqrt{3}}{\pi} \sqrt{m^2 + mn + n^2}, \quad (8.3)$$

where a_o = C–C bond length, which is equal to 1.42 Å.

The chirality of a carbon nanotube has a significant influence on its electrical and mechanical properties. Depending on the chirality, a carbon nanotube can behave either as a metallic material or a semiconducting material. For example, armchair nanotubes are metallic; nanotubes with $(n-m) = 2k$, where k is a nonzero integer, are semiconductors with a tiny band gap, and all other nanotubes are semiconductors with a band gap that inversely varies with the nanotube diameter. Chirality also controls the deformation characteristics of carbon nanotubes subjected to tensile stresses and therefore, determines whether they will fracture like a brittle material or deform like a ductile material [16].

The current processing methods used for making carbon nanotubes introduce two types of defect in their structures: topological defects and structural defects. The examples of topological defects are pentagonal and heptagonal arrangements of carbon atoms, which may be mixed with the hexagonal arrangements. The structural defects include nontubular configurations, such as cone-shaped end caps, bent shapes, branched construction with two or more tubes connected together, and bamboo-like structure in which several nanotubes are joined in the lengthwise direction. In general, MWNTs contain more defects than SWNTs.

Carbon nanotubes can form secondary structures. One of these secondary structures is the SWNT rope or bundle, which is a self-assembled close-packed array of many (often thousands or more) SWNTs. The self-assembly occurs at the time of forming the SWNTs, due to the attractive forces between them arising from binding energy of 500–900 eV/nm. If the arrangement of SWNTs in the array is well ordered (e.g., with hexagonal lattice structure), it is called a rope. If the arrangement of SWNTs is not ordered, it is called a bundle [17].

8.3.2 PRODUCTION OF CARBON NANOTUBES

There are three main methods for producing carbon nanotubes: electric arc discharge, laser ablation, and chemical vapor deposition (CVD) [18]. The quantity of production of carbon nanotubes by the first two methods is relatively small. Since CVD can produce larger quantities of carbon nanotubes and is more versatile, it has become the focus of attention for industrial production and several different variations of the basic CVD process (e.g., plasma-enhanced CVD or PECVD process and high-pressure carbon monoxide or HiPco process) have been developed. However, the structure of nanotubes produced by CVD is usually different from that of nanotubes

produced by the other two methods. For example, the CVD-produced MWNTs are less crystalline and contain more defects than the arc-discharged MWNTs. The CVD-produced MWNTs are longer and less straight than the arc-discharged MWNTs.

The arc discharge method uses two graphite rods; one serving as the cathode and the other serving as the anode, in either helium, argon, or a mixture of helium and argon atmosphere. The graphite rods are placed side by side with a very small gap, typically about 1 mm in size, between them. The pressure inside the reaction chamber is maintained between 100 and 1000 torr. When a stable arc is produced in the gap by passing 50–120 A electric current (at 12–25 V) between the graphite rods, the material eroded from the anode is deposited on the cathode in the form of MWNTs, amorphous carbon, and other carbon particles. To produce SWNTs, the cathode is doped with a small amount of metallic catalyst (Fe, Co, Ni, Y, or Mo). However, the yield of SWNTs is only between 20% and 40% by weight.

The laser ablation method uses either pulsed or continuous-wave laser to vaporize a graphite target held at 1200°C in a controlled atmosphere of argon or helium inside a tube furnace. The vaporized material is collected on a water-cooled copper collector in the form of carbon nanotubes, amorphous carbon, and other carbon particles. To produce SWNTs, the graphite target is doped with metal catalysts such as nickel and cobalt catalysts. The yield of SWNTs is between 20% and 80% by weight.

In the basic CVD method, carbon nanotubes are produced by the decomposition of a carbon-containing gas, such as carbon monoxide and hydrocarbon gases, or by the pyrolysis of carbon-containing solids, such as polymers, at a high pressure inside a furnace. The temperature inside the furnace is typically between 300°C and 800°C for making MWNTs, and 600°C and 1200°C for making SWNTs. MWNTs are produced in an inert gas atmosphere, whereas a mixture of hydrogen and an inert gas is used for SWNTs. A high-temperature substrate, such as alumina, coated with catalyst particles, such as Fe, Ni, and Co, is placed in the furnace. The decomposition of the carbon-containing gas flowing over the substrate causes the growth of carbon nanotubes on the substrate. They are collected after cooling the system down to room temperature. Depending on the carbon-containing gas, catalyst, furnace temperature, pressure, flow rate, residence time for thermal decomposition, and so on, the yield can be between 30% and 99% by weight.

All three production methods produce carbon nanotubes that are contaminated with impurities such as amorphous carbon, carbon soot, other carbon particles, and metal catalysts. Several purification processes have been developed to produce cleaner carbon nanotubes. Two of the processes are gas phase oxidation and liquid phase purification. Purification of MWNTs by gas phase oxidation involves heating them in an oxygen or air atmosphere at temperatures >700°C. In the case of SWNT, it involves heating in a mixed atmosphere of hydrochloric acid, chlorine, and water vapor at 500°C.

Liquid phase purification involves refluxing in an acid such as nitric acid at an elevated temperature. In general, carbon nanotubes produced by the arc discharge process requires more extensive purification than the other two processes.

Carbon nanotubes are often formed as long, entangled bundles. The “cutting” process is used to shorten their lengths, disentangle them, open up the ends, and provide active sites for functionalization. The cutting process can be either mechanical (e.g., by ball-milling) or chemical (e.g., by treating them in a 3:1 mixture of concentrated sulfuric acid and nitric acid).

Carbon nanotubes are available in a variety of forms. One of these forms is called the bucky paper, which is a thin film of randomly oriented SWNTs. It is made by filtering SWNTs dispersed in an aqueous or organic solution and then peeling off the nanotube film from filter paper. Carbon nanotube fibers and yarns containing aligned SWNTs have also been produced [19].

8.3.3 FUNCTIONALIZATION OF CARBON NANOTUBES

Carbon nanotubes are functionalized for a variety of purposes. Among them are (1) improve their dispersion in the polymer matrix, (2) create better bonding with the polymer matrix, and (3) increase their solubility in solvents. Functionalization has also been used for joining of nanotubes to form a network structure.

Functionalization can occur either at the defect sites on the nanotube wall or at the nanotube ends. The functional groups are covalently bonded to the nanotubes using either oxidation, fluorination, amidation, or other chemical reactions. Functionalization can also be achieved using noncovalent interactions, for example, by wrapping the nanotubes with polymer molecules or adsorption of polymer molecules in the nanotubes. The covalent functionalization is generally considered to provide better load transfer between the nanotubes and the surrounding polymer matrix, and therefore, improved mechanical properties. On the other hand, noncovalent functionalization may be preferred if it is required that the electronic characteristics of carbon nanotubes remain unchanged.

The covalent bonds can be produced in two different ways: (1) by direct attachment of functional groups to the nanotubes and (2) by a two-step functionalization process in which the nanotubes are chemically treated first to attach simple chemical groups (e.g., $-\text{COOH}$ and $-\text{OH}$) at the defect sites or at their ends (Figure 8.7), which are later substituted with more active organic groups. Carbon nanotubes have also been functionalized using silane-coupling agents [20]. Silane-coupling agents are described in Chapter 2.

A variety of chemical and electrochemical functionalization processes have been developed [15]. One of these processes is a two-step functionalization process in which acidic groups, such as the carboxylic ($-\text{COOH}$) groups or the hydroxyl ($-\text{OH}$) groups, are first attached by refluxing carbon nanotubes in concentrated HNO_3 or a mixture of H_2SO_4 and HNO_3 . One problem in acid

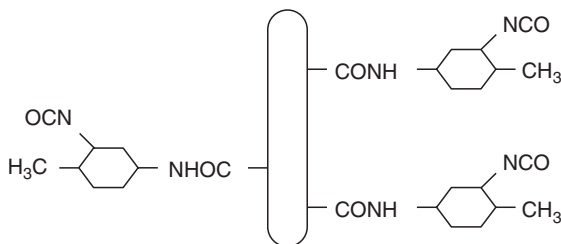


FIGURE 8.7 Schematic of a functionalized SWNT.

refluxing is that it also tends to cut the nanotubes to shorter lengths, thus reducing the fiber aspect ratio. Other milder treatments have also been developed; one of them is the ozone treatment. The ozonized surface can be reacted with several types of reagents, such as hydrogen peroxide, to create the acidic group attachments. In the second step of this process, the carbon nanotubes containing the acidic groups are subjected to amidation reaction either in a mixture of thionyl chloride (SOCl_2) and dimethyl formamide or directly in presence of an amine. The second step produces amide functionality on carbon nanotubes that are more reactive than the acid groups.

8.3.4 MECHANICAL PROPERTIES OF CARBON NANOTUBES

Theoretical calculations for defect-free carbon nanotubes show that the Young's modulus of 1–2 nm diameter SWNT is ~ 1 TPa and that of MWNT is between 1.1 and 1.3 TPa (Table 8.3). The Young's modulus of SWNT is independent of tube chirality, but it decreases with increasing diameter. The Young's

TABLE 8.3
Properties of Carbon Nanotubes

	Young's Modulus (GPa)	Tensile Strength (GPa)	Density (g/cm^3)
SWNT	1054 ^a	75 ^a	1.3
SWNT Bundle	563		1.3
MWNT	1200 ^a		2.6
Graphite (in-plane)	350	2.5	2.6
P-100 Carbon fiber	758	2.41	2.15

Note: 1 TPa = 10^3 GPa.

^a Theoretical values.

modulus of MWNT is higher than that of SWNT due to contributions from the van der Waals forces between the concentric SWNTs in MWNT [14].

Experimental determination of the mechanical properties of carbon nanotubes is extremely difficult and has produced a variety of results. Several investigators have used atomic force microscope (AFM) to determine the Young's modulus and strength. The Young's modulus of MWNT determined on AFM has ranged from 0.27 to 1.8 TPa and that of SWNT ranges from 0.32 to 1.47 TPa. Similarly, the strength of MWNT ranges from 11 to 63 GPa and that of SWNT from 10 to 52 GPa. In the TPM experiments, the carbon nanotubes have also shown high tensile strain (up to 15%) before fracture. It has also been observed that carbon nanotubes exhibit nonlinear elastic deformation under tensile, bending, as well as twisting loads. At high strains, they tend to buckle of the wall.

The large variation in Young's modulus and strength is attributed to the fact that nanotubes produced by the current production methods may vary in length, diameter, number of walls, chirality, and even atomic structure [21]. Furthermore, nanotubes produced by different methods contain different levels of defects and impurities, which influence their mechanical properties. For example, the Young's modulus of CVD-produced MWNTs is found to be an order of magnitude lower than that of the arc-discharged MWNTs, which is due to the presence of higher amount of defects in the CVD-produced MWNTs.

8.3.5 CARBON NANOTUBE-POLYMER COMPOSITES

The three principal processing methods for combining carbon nanotubes with polymer matrix [22,23] are (1) in situ polymerization, (2) solution processing, and (3) melt processing.

1. *In Situ Polymerization*: In this process, the nanotubes are first dispersed in the monomer and then the polymerization reaction is initiated to transform the monomer to polymer. Depending on the polymer formed and the surface functionality of the nanotubes, the polymer molecules are either covalently bonded to the nanotubes or wrapped around the nanotubes at the completion of the polymerization reaction.
2. *Solution Processing*: In this process, the nanotubes are mixed with a polymer solution, which is prepared by dissolving the polymer in a suitable solvent. The mixing is done using magnetic stirring, high shear mixing, or sonication. The dispersion of the nanotubes in the solution can be improved by treating them with a surfactant, such as derivatives of sodium dodecylsulfate. The solution is poured in a casting mold and the solvent is allowed to evaporate. The resulting material is a cast film or sheet of carbon nanotube-reinforced polymer.
3. *Melt Processing*: Melt processing is the preferred method for incorporating carbon nanotubes in thermoplastics, particularly for high volume

applications. It has been used with a variety of thermoplastics, such as high-density polyethylene, polypropylene, polystyrene, polycarbonate, and polyamide-6. In this process, the nanotubes are blended with the liquid polymer in a high shear mixer or in an extruder. The blend is then processed to produce the final product using injection molding, extrusion, or compression molding. It is important to note that the addition of carbon nanotubes increases the viscosity of the liquid polymer, and therefore, proper adjustments need to be made in the process parameters to mold a good product.

Carbon nanotubes have also been used with thermoset polymers such as epoxy and vinyl ester. They are dispersed in the liquid thermoset prepolymer using sonication. After mixing the blend with a hardener or curing initiator, it is poured into a casting mold, which is then heated to the curing temperature. Curing can be conducted in vacuum to reduce the void content in the composite. To improve the dispersion of the nanotubes, the viscosity of the thermoset prepolymer can be reduced with a solvent that can be evaporated later.

8.3.6 PROPERTIES OF CARBON NANOTUBE–POLYMER COMPOSITES

Based on the mechanical properties of carbon nanotubes described in Section 8.3.4, it is expected that the incorporation of carbon nanotubes in a polymer matrix will create composites with very high modulus and strength. Indeed, many studies have shown that with proper dispersion of nanotubes in the polymer matrix, significant improvement in mechanical properties can be achieved compared with the neat polymer. Three examples are given as follows.

In the first example, CVD-produced MWNTs were dispersed in a toluene solution of polystyrene using an ultrasonic bath [24]. The mean external diameter of the MWNTs was 30 nm and their length was between 50 and 55 μm . No functionalization treatments were used. MWNT-reinforced polystyrene film was produced by solution casting. Tensile properties of the solution cast films given in [Table 8.4](#) show that both elastic modulus and tensile strength increased with increasing MWNT weight fraction. With the addition of 5 wt% MWNT, the elastic modulus of the composite was 120% higher and the tensile strength was 57% higher than the corresponding properties of polystyrene.

The second example involves melt-processed MWNT-reinforced polyamide-6 [25]. The MWNTs, in this example, was also prepared by CVD and functionalized by treating them in nitric acid. The MWNTs and polyamide-6 were melt-compounded in a twin-screw mixer and film specimens were prepared by compression molding. The MWNT content in the composite was 1 wt%. As shown in [Table 8.5](#), both tensile modulus and strength of the composite were significantly higher compared with the tensile modulus and strength of polyamide-6. However, the elongation at break was decreased.

TABLE 8.4
Tensile Properties of Cast MWNT–Polystyrene

	Elastic Modulus (GPa)	Tensile Strength (MPa)
Polystyrene	1.53	19.5
Polystyrene + 1 wt% MWNT	2.1	24.5
Polystyrene + 2 wt% MWNT	2.73	25.7
Polystyrene + 5 wt% MWNT	3.4	30.6

Source: From Safadi, B., Andrews, R., and Grulke, E.A., *J. Appl. Polym. Sci.*, 84, 2660, 2002.

Note: Average values are shown in the table.

The final example considers the tensile properties of 1 wt% MWNT-reinforced epoxy [26]. The MWNT, in this case, was produced by the CVD process, and had an average diameter of 13 nm and an average length of 10 μm . They were acid-treated in a 3:1 mixture of 65% H_2SO_4 and HNO_3 for 30 min at 100°C to remove the impurities. The acid-treated nanotubes were then subjected to two different functionalization treatments: amine treatment and plasma oxidation. The acid-treated and amine-treated MWNTs were first mixed with ethanol using a sonicator and then dispersed in epoxy. The plasma-oxidized MWNTs were dispersed directly in epoxy. The composite was prepared by film casting. As shown in Table 8.6, the addition of MWNT caused very little improvement in modulus, but tensile strength and elongation at break were significantly improved.

TABLE 8.5
Tensile Properties of 1 wt% MWNT-Reinforced Polyamide-6

	Polyamide-6	1 wt% MWNT +Polyamide-6
Tensile modulus (GPa)	0.396	0.852
Yield strength (MPa)	18	40.3
Elongation at break	>150	125

Source: From Zhang, W.D., Shen, L., Phang, I.Y., and Liu, T., *Macromolecules*, 37, 256, 2004.

Note: Average values are shown in the table.

TABLE 8.6
Tensile Properties of 1 wt% MWNT–Epoxy Composites

	Young's Modulus (GPa)	Tensile Strength (MPa)	Elongation at Break (%)
Epoxy	1.21	26	2.33
Untreated MWNT–epoxy	1.38	42	3.83
Acid-treated MWNT–epoxy	1.22	44	4.94
Amine-treated MWNT–epoxy	1.23	47	4.72
Plasma-treated MWNT–epoxy	1.61	58	5.22

Source: From Kim, J.A., Seong, D.G., Kang, T.J., and Youn, J.R., *Carbon*, 44, 1898, 2006.

Note: Average values are shown in the table.

The three examples cited earlier are among many that have been published in the literature. They all show that the addition of carbon nanotubes, even in small concentrations, is capable of improving one or more mechanical properties of polymers. Thermal properties, such as thermal conductivity, glass transition temperature, and thermal decomposition temperature, and electrical properties, such as electrical conductivity, are also increased. However, several problems have been mentioned about combining nanotubes with polymers and achieving the properties that carbon nanotubes are capable of imparting to the polymer matrix. The most important of them are nanotube dispersion and surface interaction with the polymer matrix [22,23]. For efficient load transfer between the nanotubes and the polymer, they must be dispersed uniformly without forming agglomeration. Relatively good dispersion can be achieved with proper mixing techniques (such as ultrasonication) at very small volume fractions, typically less than 1%–2%. At larger volume fractions the nanotubes tend to form agglomeration, which is accompanied by decrease in modulus and strength.

One contributing factor to poor dispersion is that the carbon nanotubes (and other nano-reinforcements) have very high surface area and also very high length-to-diameter ratio [27,28]. While both provide opportunity for greater interface interaction and load transfer, the distance between the individually dispersed nanotubes becomes so small even at 10% volume fraction that the polymer molecules cannot infiltrate between them. Strong attractive forces between the nanotubes also contribute to poor dispersion. This is particularly true with SWNTs, which tend to form bundles (nanoropes) that are difficult to separate. MWNTs, in general, exhibit better dispersion than SWNTs.

The surface interaction between the carbon nanotubes and the polymer matrix requires good bonding between them, which is achieved by functionalization of nanotubes. Functionalization also helps improve the dispersion of nanotubes in the polymer. Table 8.6 shows the effect of functionalization

TABLE 8.7
Tensile Properties of Functionalized SWNT-Reinforced Polyvinyl Alcohol (PVA) Film

Material	Young's Modulus (GPa)	Yield Strength (MPa)	Strain-to-Failure (mm/mm)
PVA	4.0	83	>0.60
PVA + 2.5% purified SWNT	5.4	79	0.09
PVA + 2.5% functionalized SWNT	5.6	97	0.05
PVA + 5% functionalized SWNT	6.2	128	0.06

Source: From Paiva, M.C., Zhou, B., Fernando, K.A.S., Lin, Y., Kennedy, J.M., and Sun, Y.-P., *Carbon*, 42, 2849, 2004.

Note: Average values are shown in the table.

of MWNTs. The effect of functionalization of SWNT is shown in Table 8.7, which gives the tensile properties of functionalized SWNT-reinforced PVA. In this case, the SWNTs were prepared by the arc discharge method and purified by refluxing in an aqueous nitric acid solution. The nanotubes were then functionalized with low-molecular-weight PVA [29] using *N,N'*-dicyclohexyl carbodiimide-activated esterification reaction. The functionalized SWNTs were mixed with a water solution of PVA and solution cast into 50–100 μm thick films. Both Young's modulus and yield strength were significantly higher with functionalized SWNTs. The higher yield strength with 2.5 wt% functionalized SWNTs compared with 2.5 wt% purified SWNTs (without functionalization) was attributed to deagglomeration of SWNT ropes into separate nanotubes, better dispersion of them in the PVA matrix, and wetting by PVA.

Another approach to improving the mechanical properties of carbon nanotube-reinforced polymers is to align the nanotubes in the direction of stress. This is a relatively difficult task if the common processing methods are used. Flow-induced alignment of nanotubes is created by solution spinning, melt spinning, or other similar methods to produce carbon nanotube-reinforced polymer fiber or film. Mechanical stretching of carbon nanotube-reinforced thin polymer films also tend to align the nanotubes in the direction of stretching. Other methods of aligning carbon nanotubes in polymer matrix, including the application of magnetic field, are described in Ref. [23].

The effect of alignment of nanotubes on the properties of carbon nanotube-reinforced polymer fibers is demonstrated in Table 8.8. In this case, the polymer was polyacrylonitrile (PAN) and the fibers were prepared by solution spinning [30]. The carbon nanotube content was 5% by weight. All of the mechanical properties, including strain-at-failure and toughness, increased with the addition of SWNT, MWNT, as well as VGCNF. There was a significant decrease

TABLE 8.8
Properties of SWNT, MWNT, and VGCNF-Reinforced PAN Fibers

	PAN Fiber	(PAN + SWNT) Fiber	(PAN + MWNT) Fiber	(PAN + VGCNF) Fiber
Modulus (GPa)	7.8	13.6	10.8	10.6
Strength at break (MPa)	244	335	412	335
Strain-at-failure (%)	5.5	9.4	11.4	6.7
Toughness (MN m/m ³)	8.5	20.4	28.3	14
Shrinkage (%) at 160°C	13.5	6.5	8.0	11.0
T _g (°C)	100	109	103	103

Source: From Chae, H.G., Sreekumar, T.V., Uchida, T., and Kumar, S., *Polymer*, 46, 10925, 2005.

Note: Average values are shown in the table.

in thermal shrinkage and increase in the glass transition temperature (T_g). The improvements in the properties were not only due to the alignment of nano-reinforcements in the fiber, but also due to higher orientation of PAN molecules in the fiber caused by the presence of nano-reinforcements.

REFERENCES

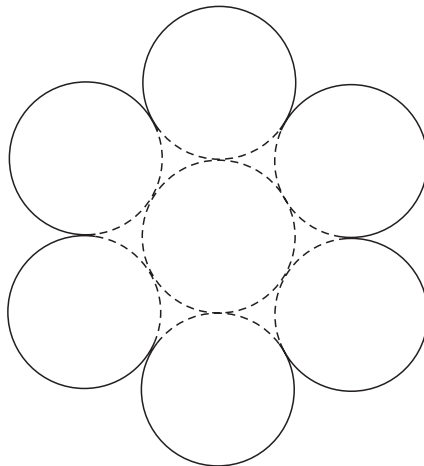
1. M. Alexandre and P. Dubois, Polymer-layered silicate nanocomposites: preparation, properties and uses of a new class of materials, *Mater. Sci. Eng.*, 28:1 (2000).
2. M. Kato and A. Usuki, Polymer-clay nanocomposites, in *Polymer-Clay Nanocomposites* (T.J. Pinnavaai and G.W. Beall, eds.), John Wiley & Sons, Chichester, UK (2000).
3. H.R. Dennis, D.L. Hunter, D. Chang, S. Kim, J.L. White, J.W. Cho, and D.R. Paul, Effect of melt processing conditions on the extent of exfoliation in organoclay-based nanocomposites, *Polymer*, 42:9513 (2001).
4. S.J. Ahmadi, Y.D. Huang, and W. Li, Synthetic routes, properties and future applications of polymer-layered silicate nanocomposites, *J. Mater. Sci.*, 39:1919 (2004).
5. G.G. Tibbetts, M.L. Lake, K.L. Strong, and B.P. Price, A review of the fabrication and properties of vapor-grown carbon nanofiber/polymer composites, *Composites Sci. Tech.* 67:1709 (2007).
6. I.S. Chronakis, Novel nanocomposites and nanoceramics based on polymer nanofibers using electrospinning technology, *J. Mater. Process. Tech.*, 167:283 (2005).
7. Y.-Y. Fan, H.-M. Cheng, Y.-L. Wei, G. Su, and Z.-H. Shen, Tailoring the diameters of vapor-grown carbon nanofibers, *Carbon*, 38:921 (2000).
8. J.-H. Zhou, Z.-J. Sui, P. Li, D. Chen, Y.-C. Dai, and W.K. Yuan, Structural characterization of carbon nanofibers formed from different carbon-containing gases, *Carbon*, 44:3255 (2006).
9. O.C. Carnerio, N.M. Rodriguez, and R.T.K. Baker, Growth of carbon nanofibers from the iron-copper catalyzed decomposition of CO/C₂H₄/H₂ mixtures, *Carbon*, 43:2389 (2005).

10. T. Uchida, D.P. Anderson, M. Minus, and S. Kumar, Morphology and modulus of vapor grown carbon nano fibers, *J. Mater. Sci.*, 41:5851 (2006).
11. F.W.J. van Hattum, J.M. Benito-Romero, A. Madronero, and C.A. Bernardo, Morphological, mechanical and interfacial analysis of vapour-grown carbon fibres, *Carbon*, 35:1175 (1997).
12. I.C. Finegan, G.G. Tibbetts, D.G. Glasgow, J.-M. Ting, and M.L. Lake, Surface treatments for improving the mechanical properties of carbon nanofiber/thermo-plastic composites, *J. Mater. Sci.*, 38:3485 (2003).
13. R.D. Patton, C.U. Pittman, Jr., L. Wang, and J.R. Hill, Vapor grown carbon fiber composites with epoxy and poly(phenylene sulfide) matrices, *Composites: Part A*, 30:1081 (1999).
14. J. Han, Structure and properties of carbon nanotubes, *Carbon Nanotubes: Science and Applications* (M. Meyappan, ed.), CRC Press, Boca Raton, USA (2005).
15. E.G. Rakov, Chemistry of carbon nanotubes, *Nanomaterials Handbook* (Y. Gogotsi, ed.), CRC Press, Boca Raton, USA, pp. 105–175 (2006).
16. E.T. Thostenson, Z. Ren, and T.-W. Chou, Advances in the science and technology of carbon nanotubes and their composites, *Compos. Sci. Tech.*, 61:1899 (2001).
17. J.E. Fischer, Carbon nanotubes: structure and properties, *Nanomaterials Handbook* (Y. Gogotsi, ed.), CRC Press, Boca Raton, USA, pp. 69–103 (2006).
18. D. Mann, Synthesis of carbon nanotubes, *Carbon Nanotubes: Properties and Applications* (M.J. O'Connell, ed.), CRC Press, Boca Raton, USA, pp. 19–49 (2006).
19. H.G. Chae, J. Liu, and S. Kumar, Carbon nanotube-enabled materials, *Carbon Nanotubes: Properties and Applications* (M.J. O'Connell, ed.), CRC Press, Boca Raton, USA, pp. 19–49 (2006).
20. P.C. Ma, J.-K. Kim, and B.Z. Tang, Functionalization of carbon nanotubes using a silane coupling agent, *Carbon*, 44:3232 (2006).
21. N. Grobert, Carbon nanotubes—becoming clean, *Mater. Today*, 10:28 (2007).
22. J.N. Coleman, U. Khan, W.J. Blau, and Y.K. Gun'ko, Small but strong: a review of the mechanical properties of carbon nanotube–polymer composites, *Carbon*, 44:1624 (2006).
23. X.-L. Xie, Y.-W. Mai, and X.-P. Zhou, Dispersion and alignment of carbon nanotubes in polymer matrix: a review, *Mater. Sci. Eng.*, R49:89 (2005).
24. B. Safadi, R. Andrews, and E.A. Grulke, Multiwalled carbon nanotube polymer composites: synthesis and characterization of thin films, *J. Appl. Polym. Sci.*, 84:2660 (2002).
25. W.D. Zhang, L. Shen, I.Y. Phang, and T. Liu, Carbon nanotubes reinforced nylon-6 composite prepared by simple melt compounding, *Macromolecules*, 37:256 (2004).
26. J.A. Kim, D.G. Seong, T.J. Kang, and J.R. Youn, Effects of surface modification on rheological and mechanical properties of CNT/epoxy composites, *Carbon*, 44:1898 (2006).
27. F.H. Gojny, M.H.G. Wichmann, B. Fiedler, and K. Schulte, Influence of different carbon nanotubes on the mechanical properties of epoxy matrix composites—a comparative study, *Compos. Sci. Tech.*, 65:2300 (2005).
28. B. Fiedler, F.H. Gojny, M.H.G. Wichmann, M.C.M. Nolte, and K. Schulte, Fundamental aspects of nano-reinforced composites, *Compos. Sci. Tech.*, 66:3115 (2006).

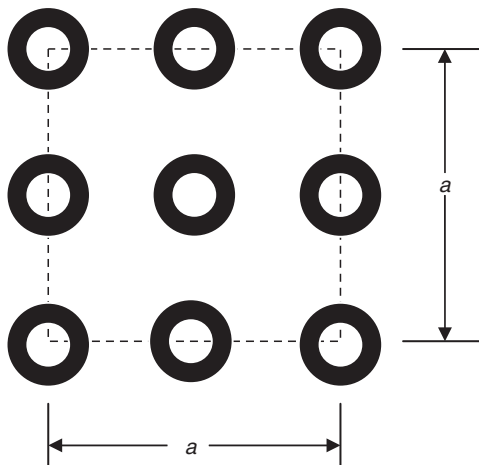
29. M.C. Paiva, B. Zhou, K.A.S. Fernando, Y. Lin, J.M. Kennedy, and Y.-P. Sun, Mechanical and morphological characterization of polymer–carbon nanocomposites from functionalized carbon nanotubes, *Carbon*, 42:2849 (2004).
30. H.G. Chae, T.V. Sreekumar, T. Uchida, and S. Kumar, A comparison of reinforcement efficiency of various types of carbon nanotubes in polyacrylonitrile fiber, *Polymer*, 46:10925 (2005).

PROBLEMS

- P8.1. Calculate the specific surface area (unit: m^2/g) of a defect-free single-walled carbon nanotube (SWNT) assuming that the length of the C–C bonds in the curved graphite sheet is the same as that in a planar sheet, which is 0.1421 nm. The atomic mass of carbon is 12 g/mol and the Avogadro’s number is 6.023×10^{23} per mole. Assume that the surface area of the end caps is negligible compared with the surface area of the cylindrical side wall.
- P8.2. Using the information given in Problem P8.1, calculate the specific surface area of a defect-free double-walled carbon nanotube (DWNT).
- P8.3. The specific surface area of SWNT is independent of the nanotube diameter, whereas the specific surface area of MWNT decreases with the nanotube diameter. Why?
- P8.4. Assume that SWNTs in a nanorope are arranged in a regular hexagonal array as shown in the following figure. Using the information given in Problem P8.1, calculate the specific surface area of the nanorope.



- P8.5. Assume that the carbon nanotubes in a nanotube–polymer composite are arranged in a regular face-centered square array as shown in the following figure. Calculate the distance between the nanotubes as a function of nanotube volume fraction. Knowing that the polymer molecules are 0.8 nm in diameter, discuss the problem of incorporating high nanotube concentration in a polymer matrix.



- P8.6. In Table 8.8, the tensile modulus of SWNT-reinforced polyacrylonitrile (PAN) fibers is reported as 13.6 GPa. The SWNTs were dispersed in these fibers as bundles and the average bundle diameter was 10 nm. The average length of the SWNT bundles was 300 nm and the SWNT volume fraction was 4.6%.
- Using the Halpin–Tsai equations (Appendix A.4) and assuming that the SWNT bundles were aligned along the fiber length, calculate the theoretical modulus of the SWNT-reinforced polyacrylonitrile fiber. The modulus of PAN fibers, $E_{\text{PAN}} = 7.8$ GPa and the modulus of SWNT, $E_{\text{SWNT}} = 640$ GPa.
 - What may be the principal reasons for the difference between the theoretical modulus and the experimentally determined modulus of 13.6 GPa?
 - How will the theoretical modulus change if the SWNT bundles were completely exfoliated into individual SWNTs of 1.2 nm diameter?

